# Prism-based ultrafast pulse-shaping apparatus

**Emmanouil Lioudakis**
**Katerina Adamou**
**Andreas Othonos**
University of Cyprus
Department of Physics
P.O. Box 20537
1678, Nicosia, Cyprus
E-mail: othonos@ucy.ac.cy

**Abstract.** We report on a computer-controlled pulse-shaper setup with high-efficiency throughput, based on dispersive prisms, as an alternative to the conventional grating ultrafast pulse-shaping apparatus. A detailed description of the experimental apparatus and operation of this system is given. The advantages and disadvantages of this configuration are discussed. Experimental implementation of the prism pulse shaper in recovering nearly bandwidth-limited laser pulses from chirped ultrafast laser pulses is demonstrated using both closed-loop and open-loop operation.
 [DOI: 10.1117/1.1873432]

Subject terms: ultrafast laser pulses; pulse shaper; dispersive prisms.

Paper 040520 received Aug. 2, 2004; revised manuscript received Oct. 12, 2004; accepted for publication Oct. 13, 2004; published online Mar. 4, 2005.

## 1 Introduction

Ultrafast science has been at the forefront of photonics and optoelectronics technology over the past 2 decades. Breakthroughs in generating shorter pulses as well as controlling the electric field of such pulses have been the subject of a great deal of research. Recently the realization of electronic modulation and eventually the shaping of ultrashort pulses has found applications in most fields of science. Numerous modulation schemes for shaping ultrafast laser pulses have been proposed.[1–3] The most common arrangement, which was initially proposed by Weiner et al.[4] is known as the ''zero-dispersion compressor.'' This configuration is a $4f$ geometry pulse shaper that is composed of a pair of diffraction gratings and a pair of achromatic lenses (or mirrors).[1,5] The pulse shaper has been used in combination with a Ti:sapphire oscillator[6] as well as with amplified laser systems,[7] and it has shown promising results.[8,9] The main component that revolutionized the pulse shaper is a programmable electro-optic spatial light modulator (SLM), which replaces the microlithographic masks and offers a number of advantages. Recent demonstrations have shown the capability of shaping ultrafast pulses using two independent control techniques, known as open- and closed-loop strategies. In an open-loop operation, the pulse-shaping apparatus offers control of the phase and amplitude, resulting in the desired optical waveform synthesis. In a closed-loop operation, an adaptive feedback-learning algorithm can be used as a means to control the shape of the output laser pulse and its interaction with matter.[10–13]

The conventional pulse-shaping apparatus requires careful design considerations of the various optical elements utilized in the setup. Of particular importance are the gratings used to disperse the incident ultrafast laser pulse in combination with the focusing optics. Physical restrictions to the pulse shaper setup may not allow efficient use of the gratings. Furthermore, the efficiency of such gratings greatly depends on the wavelength and pulse width of the incident laser pulse; values that may be required to change under certain experimental conditions, resulting in a low grating efficiency. For example, in a $4$-$f$ geometry setup, where the ultrafast laser pulse is centered at 840 nm, bandwidth of 45 nm FWHM and focusing optics of 12 cm focal length (shorter focal length is mechanically restricted), the gratings efficiency will be 30%, resulting in a throughput of approximately 10% of the incident laser energy in the pulse-shaping apparatus. This energy throughput value may be prohibiting to some experiments, especially those involving only a simple laser oscillator.

## 2 Prism-Based Pulse-Shaping Apparatus

In this paper, we demonstrate the use of a simple prism-based configuration for shaping ultrafast pulses as an alternative technique to the conventional grating-based pulse shaper.[1] This alternative setup alleviates some of the drawbacks of the conventional pulse-shaping apparatus, with noticeable improvements on the energy throughput of the system. This high-efficiency pulse shaper can modulate the phase and amplitude of the electric field of the pulse. The alignment of the apparatus is simple and consists of optical elements that most laboratories involved in ultrafast work already posses for dispersion compensation. Finally, the system, as in the case of the conventional pulse shaper, can be combined with adaptive closed-loop control experiments in many fields of ultrafast spectroscopy, physical chemistry, communications, and semiconductors physics. Here we report on the characteristics and operation of this high-efficiency prism-based pulse-shaper setup. Ultrafast techniques such as frequency-resolved optical gating (FROG) are utilized to obtain a complete picture of the laser pulse electric field, and thus a better understanding of the behavior of the pulse-shaper system. Furthermore, to demonstrate the operation of this prism-based pulse shaper a genetic algorithm is employed in a closed-loop configuration to compress a laser pulse from a Ti:sapphire oscillator with complex phase distortion, and the results are analyzed in detail.

Figure 1 shows the layout of our simple programmable femtosecond pulse-shaping setup, which consists of two pairs of prisms and a liquid crystal display. The arrangement is the typical dispersion compensation setup often utilized in ultrafast laser work. We use a home-built Ti:sapphire oscillator to generate approximately 40-fs pulses at a center wavelength of 840 nm with output power 350 mW

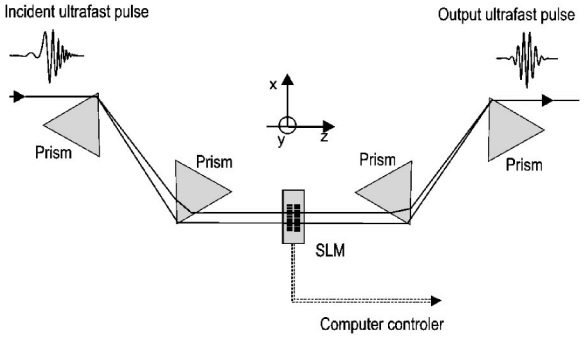


**Fig. 1** Basic arrangement of a prism-based programmable pulse-shaping system for ultrafast laser pulses.

and a repetition rate of 100 MHz. The output pulses strike the first prism where different wavelengths emerge at different angles and then they are incident on the second prism of the first pair. With the laser pulse horizontally polarized and the prisms placed in a Brewster configuration, the arrangement offers the minimum losses.

In the proposed pulse-shaper configuration, the first prism serves as a dispersive element, producing group-velocity dispersion, while the second prism produces a parallel output ray. The distance between the two prisms and the total optical path length through the dispersive materials were estimated so as to maintain transform-limited pulses.[14] After the second prism, in the symmetrical plane of the system, the spatially separated spectral components can be manipulated by phase and/or amplitude masks. In our system, this is accomplished using a two-layer SLM, which is suitable for phase and/or amplitude modulation.[15] Each layer of the SLM consists of 128 separate pixels, sized 100 $\mu$m width by 2 mm height. The $z$ axis defines the direction of propagation, whereas the preferential orientation axes of the nematic liquid crystal molecules in the first and in the second SLM layers are located in the $x$-$y$ plane, rotated by $-45$ and $+45$ deg, respectively, from the $x$ axis. In our configuration, an $x$-polarized input light has polarization components of equal magnitude along these two orientation axes (1,2). If suitable voltages are applied to the separate pixels, the liquid crystal molecules are tilted in the 1-$z$ and 2-$z$ planes, respectively, thereby enabling independent changes of the refractive indices for the two corresponding light-polarization components at 128 individual wavelength intervals throughout the laser spectrum.

The modified spectrum of the pulse follows exactly the same optical path in a second antiparallel pair of prisms in a Brewster configuration. In this arrangement, the spectrum is recombined to form a collimated output beam. The temporal profile of the output field is then given by the Fourier transform of the pattern transferred by the mask onto the pulse spectrum. The major dispersion contribution from the prism arrangement consists of a negative term due to angular dispersion and a positive term due to the finite glass the beam propagates through. The sign difference in the two types of group velocity dispersion (GVD) offers the ability to adjust the total GVD through zero by translating the apexes of the prisms toward or outward with respect to the laser beam.[16] The energy throughput of our pulse-shaper setup was measured to be $\sim$97% of the incident pulse energy, not including the losses due to the SLM. The prisms used in the pulse shaper were made out of Schott SF10 glass, and the distance between them was set at 75 cm to have approximately 10-mm expansion of the beam coming out of the second prism where the SLM was placed. The spectral profile and content of the ultrafast laser beam coming out of the second prism was investigated in detail using a slit and a spectrometer. The measurements indicate a spectral resolution of 0.65 nm in 100-$\mu$m steps and an intensity profile like the original ultrafast pulse that was measured before the prism setup, confirming that the prism assembly did not affect the spectral content of our ultrafast laser pulse. Furthermore, smaller prism separations were also investigated, resulting in smaller beam expansion at the SLM position. Specifically, for prism separation of 35 cm resulting in a beam expansion covering only 45 pixels, we were able to accomplish adequate pulse shaping, however, we were not able to take full advantage of the 128 pixels this particular SLM offers. Finally, before the insertion of the SLM in the prism pulse-shaper system, the prism separation and the material the laser beam transversed were carefully adjusted with the help of FROG traces for minimum pulse width and nearly transform-limited pulses estimated to be 39 fs at FWHM. Insertion of the SLM required a minor readjustment of the prisms to compensate for the chirp introduced due to the LCD layers and polarizers of the SLM.

Note that FROG traces were obtained with the help of a homemade FROG apparatus. The system has a typical autocorrelation geometry[17,18] (based on an interferometer), where the incoming beam is divided in two equal intensity parts. One beam travels through an optical path with a fixed length and the other through a path that includes an optical delay line with the help of a retroreflector mounted on a computer-controlled translation stage. In this setup, the spatial position of the retroreflector on the translation stage is related directly to the relative time delay between the two beams of pulses. The beams from the two optical paths are focused on a BBO nonlinear crystal with a help of a short-focus lens. The spectral profile of the second-harmonic signal generated is collected and recorded with a linear array spectrometer as a function of the optical path delay. This spectra profile versus optical delay constitutes 3-D FROG traces, where phase-retrieval algorithms[18] provide detailed information about the electric field intensity and phase of the laser pulse.

## 3 Experimental Results and Discussion

In a first experimental demonstration of the prism-based pulse shaper, we placed a thick glass in front of the Ti:sapphire oscillator, introducing a complex chirp to the laser pulse, which we attempted to remove with the help of the pulse-shaper system. To characterize and compare in detail the incoming and shaped laser pulse FROG traces were recorded (Fig. 2). Figure 2(a) shows a typical FROG trace of the chirped laser pulse from the Ti:sapphire oscillator due to the dispersive thick glass. The FROG retrieval algorithm suggests that this pulse exhibits a complex high-order chirp. These complex phase distortions were eliminated using a genetic algorithm in conjunction with the pulse shaper setup. This algorithm uses as a feedback signal the second-harmonic generation (SHG) that is recorded from the

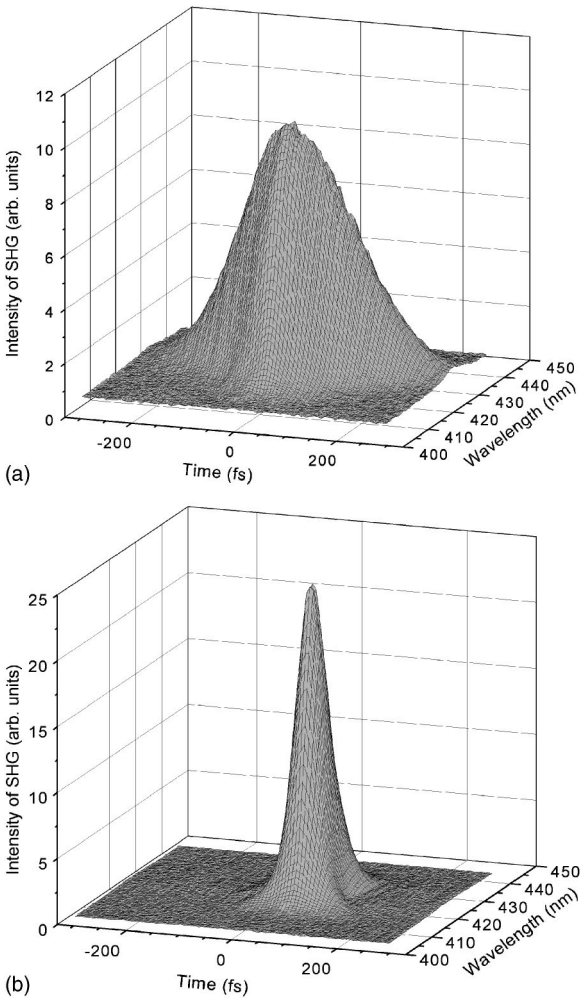


**Fig. 2** Second-harmonic FROG traces: (a) ultrafast laser pulse undergoes temporal broadening when transverse a thick glass and (b) ultrafast pulse undergoes pulse compression using a genetic algorithm in conjunction with the SLM pulse-shaper system.

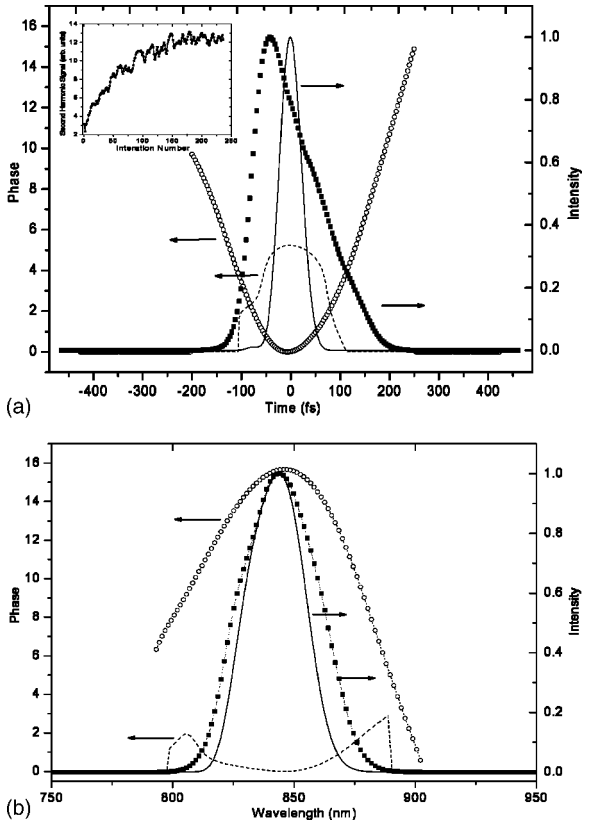


**Fig. 3** Intensity and phase profiles of the initial (represented by solid squares and open circles, respectively) and final pulse (represented by solid and dashed lines, respectively) after pulse shaping using a genetic algorithm as a function of (a) time and (b) wavelength. The information is obtained from FROG retrieval routines. The indented graph in the upper left corner is the SHG signal evolution using the genetic algorithm in a closed-loop strategy of the prism-based pulse shaper.

FROG setup. After a number of iterations, the genetic algorithm converged at the maximum SHG signal and the voltages for each pixel of both SLM layers were extracted. These voltages resulted in phase and amplitude modulation of the incoming chirped pulse. Figure 2(b) displays the FROG trace of the resultant compress laser pulse after 200 iterations. From a comparison of the two traces, the laser pulse after the genetic algorithm iterations appears to have undergone a dramatic temporal compression. This becomes clear from the retrieved intensity and phase profiles of the FROG traces in the time and wavelength domains. The incoming laser pulse intensity (solid squares) and phase (open circles) profiles as well as the intensity (solid line) and phase (dashed line) profiles of the compressed laser pulse are shown in Figs. 3(a) and 3(b). The asymmetry of the intensity profile in the time domain and the broadening in the wavelength domain of the input pulse is characteristic of cubic- and quartic-phase dispersion. This was confirmed using a polynomial fitting of the retrieved phase curve [Fig. 3(b)]. The insert in the upper left corner of Fig. 3(a) shows the evolution of the SHG signal as a function of iterations. It is clearly evident from this figure that pulse shaping using the prism-based system has reached a maximum SHG signal after 200 iterations. The initial pulse duration was found to be 135 fs at FWHM, whereas after the pulse compression process this was reduced to 43 fs at FWHM. The results show a significant reduction of the pulse duration, which approaches the Fourier-transform-limited pulse. The spectral and temporal phase indicates almost flat behavior at the region of nonvanishing intensity. Note that with the closed-loop technique, knowledge of the system response or the registration of the pixel number with the corresponding wavelength range is not required.

Next, we investigated the programmable prism-based pulse shaper in the open-loop operation. Here, one requires an accurate calibration of the SLM pixel-wavelength correspondence as well as voltage level-transmission behavior (which is also wavelength dependent). Given that laser parameters, such as center lasing wavelength and beam direction, may drift from day to day, operation calibration was performed on a daily bases once the laser has stabilized. Therefore, it became necessary to automate this procedure. This was achieved using the SLM controller and a computer-controlled CCD spectrometer. The transmission of one of the pixel arrays was set to maximum, whereas the other array was varied though all the available voltage digital levels (0 to 4095). The spectral profiles were collected

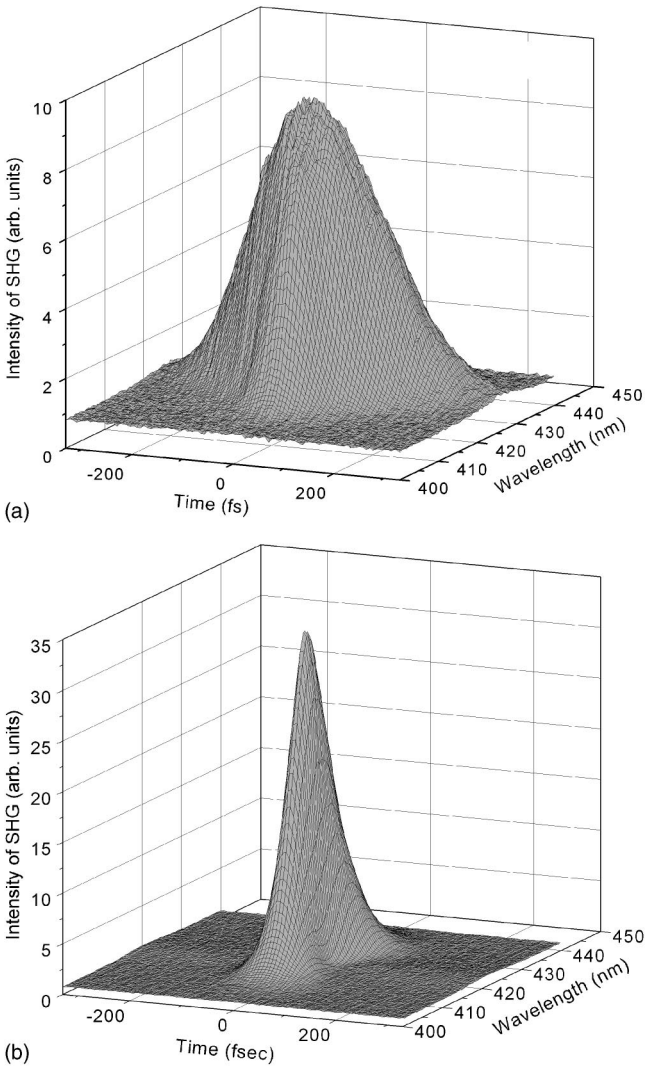


**Fig. 4** Second-harmonic FROG traces: (a) ultrafast laser pulse undergoes temporal broadening when transverse a thick glass (160 fs at FWHM) and (b) ultrafast pulse undergoes pulse compression using applied voltages on SLM following calibration of the system. The pulse was estimated at 44 fs at FWHM.

and measured. This was applied for all the pixels of the SLM, giving a complete and automated procedure for the control of the SLM. Using this information, we were able to construct calibration curves, which enabled the modification and reshaping of the output pulses from the pulse shaper. At this point, a thick optical glass was used to introduce a complex chirp into the incoming ultrashort pulse, resulting in a pulse of approximately 160 fs at FWHM [Fig. 4(a)]. Using a FROG trace from the resultant chirped pulse and the calibration curves we were able to calculate the required voltage on the SLM pixels to remove the induced chirped. Application of the estimated voltage on the SLM system resulted in the removal of the induced chirped [Fig. 4(b)] with the ultrafast pulse approaching its Fourier transform limit (44 fs at FWHM) as in the case of the closed-loop operation. The advantage in the open-loop operation of the pulse shaper, once the system has been calibrated, is that it is less time consuming than the closed-loop operation.

In view of the symmetry of the four-prism-based pulse-shaper apparatus, the system can further be simplified using a mirror after the first prism pair and the SLM. The reflected beam will be directed back at a slightly tilted angle through the SLM and the prisms, eliminating the need for the second prism pair. When using this simplified two-prism pulse-shaper system in an open-loop configuration, a more careful analysis must be considered due to the double pass of the laser pulses though the SLM. On the other hand, in a closed-loop configuration this consideration is not necessary since this is accomplished with the help of the evolutionary algorithm. Using the two-prism pulse shaper in a closed-loop configuration we were able to demonstrate pulse compression of an ultrafast-chirped laser pulse to its nearly transform limited shape following approximately 180 iterations.

Finally, a major drawback of the proposed experimental arrangement of the ultrafast pulse shaper is the relatively large distance separation between the prisms required to expand the beam to cover the maximum number of SLM elements. This problem, however, can be overcome using expanding optics. A simple telescope arrangement can be used to expand the laser beam to cover the total number of elements in the SLM, resulting in a system of smaller footprint than the conventional grating-based pulse shaper. We believe this approach will make the prism-based pulse shaper an attractive alternative over the conventional grating-based pulse shaper, especially in the case where parameters such as wavelength and pulse bandwidth must vary.

## 4 Conclusion

We reported the construction of a programmable pulse shaper, which combines a four-prism arrangement with a two-layer liquid crystal display system. This setup has a high-energy efficiency throughput; it is very simple to align and has a relatively low cost of fabrication. We demonstrated the use of the prism-based pulse shaper and its behavior using both closed-loop and open-loop operations. We believe that this new setup of optical femtosecond prism-based pulse shaping is robust and may prove to be an attractive alternative to the conventional grating-based pulse-shaper system, especially in the case where parameters such as wavelength and pulse bandwidth must vary. Finally, the high throughput efficiency of this pulse shaper makes experiments possible even with low-energy ultrafast oscillators.

### *Acknowledgments*

This work was carried out in the Photonics and Optoelectronics Research Laboratory in Cyprus and was funded by the Government of Cyprus Program (P.E.N.E.K) of the Research Promotion Foundation.

### *References*

1. A. M. Weiner, *Rev. Sci. Instrum.* **71**(5), 1929–1960 (2000).
2. A. Efimov, C. Schaffer, and D. H. Reitze, *J. Opt. Soc. Am. B* **12**(10), 1968–1980 (1995).
3. E. Zeek, K. Maginnis, S. Backus, U. Russek, M. Murnane, G. Mourou, H. Kapteyn, and G. Vdovin, *Opt. Lett.* **24**(7), 493–495 (1999).
4. A. M. Weiner, J. P. Heritage, and E. M. Kirschner, *J. Opt. Soc. Am. B* **5**(8), 1563–1572 (1988).
5. T. Brixner and G. Gerber, *Opt. Lett.* **26**(8), 557–559 (2001).

6. T. Baumert, T. Brixner, V. Seyfried, M. Strehle, and G. Gerber, *Appl. Phys. B: Lasers Opt.* **65**(6), 779–782 (1997).
7. T. Brixner, M. Strehle, and G. Gerber, *Appl. Phys. B: Lasers Opt.* **68**(2), 281–284 (1999).
8. D. Meshulach, D. Yelin, and Y. Silberderg, *J. Opt. Soc. Am. B* **15**(5), 1615–1619 (1998).
9. A. Assion, T. Baumert, M. Bergt, T. Brixner, B. Kiefer, V. Seyfried, M. Strehle, and G. Gerber, *Science* **282**(5390), 919–922 (1998).
10. J. Kunde, B. Baumann, S. Arlt, and F. Morier-Genoud, *Appl. Phys. Lett.* **77**(7), 924–926 (2000).
11. J. Kunde, U. Siegner, S. Arlt, G. Steinmeyer, F. Morier-Genoud, and U. Keller, *J. Opt. Soc. Am. B* **16**(12), 2285–2294 (1999).
12. U. Siegner, M. Haiml, J. Kunde, and U. Keller, *Opt. Lett.* **27**(5), 315–317 (2002).
13. A. Efimov, M. D. Moores, B. Mei, J. L. Krause, C. W. Siders, and D. H. Reitze, *Appl. Phys. B* **70**, S133–S141 (2000).
14. J. C. Diels and W. Rudolph, Academic, San Diego, CA (1996).
15. ''Manual of Cambridge Research & Instrumentation,'' Revision 1.01 (1996).
16. R. L. Fork, O. E. Martinez, and J. P. Gordon, *Opt. Lett.* **9**(5), 150–152 (1984).
17. A. Othonos, *J. Appl. Phys.* **84**, 1789–1830 (1998).
18. R. Trebino, *Frequency-Resoved Optical Gating: The Measurement of Ultrashort Laser Pulses*, Kluwer Academic, Boston (2000).

Biographies and photographs of authors not available.